Electronic Supporting Information for:

Deciphering the Excited State Landscape of Cr(III) *Tris*(diimines) Using $[Cr(phen)_3]^{3+}$

Alexandra T. Barth,[1†] Dilara Farkhutdinova,[2,3†] Adrienne P. Faulkner,[1] Irene Y. Dzaye,[1] Jonathan P. Wheeler,[1] Leticia González, [2*] and Felix N. Castellano[1*]

[1]*Department of Chemistry, North Carolina State University, Raleigh, North Carolina, 27695-8204, United States.*
[2]*Institute of Theoretical Chemistry, Faculty of Chemistry, University of Vienna, Währinger Straße 17, 1090 Vienna, Austria*
[3]*Doctoral School in Chemistry (DosChem), University of Vienna, Währinger Straße 38, 1090 Vienna, Austria*

[†]Denotes equal authorship contribution

1. Supporting Figures and Tables

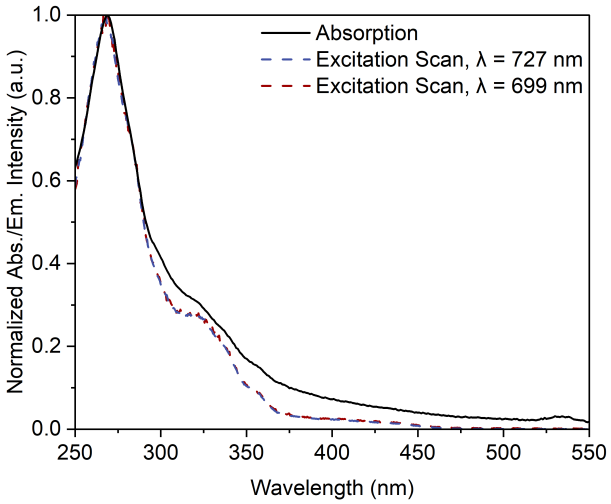

Figure S1. Normalized absorption and excitation scans from metal-centered ^2E (727 nm) and $^2T_1$ (699 nm) emission features in compound **1**. Measurements recorded at 295 K in CH_3CN.

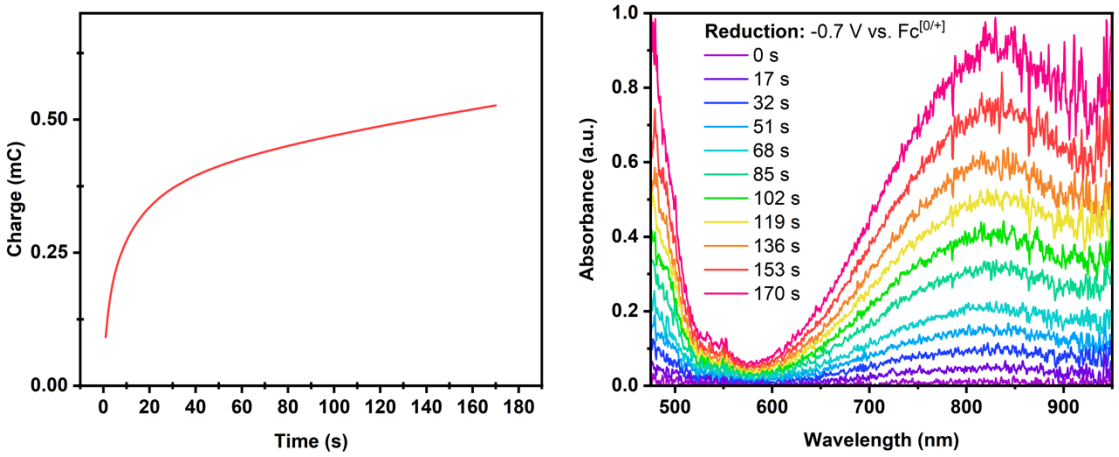

Figure S2. Spectroelectrochemistry data of compound **1** showing (left) the charge passed and (right) the change in spectral absorption profile during the first ligand-centered reduction event.

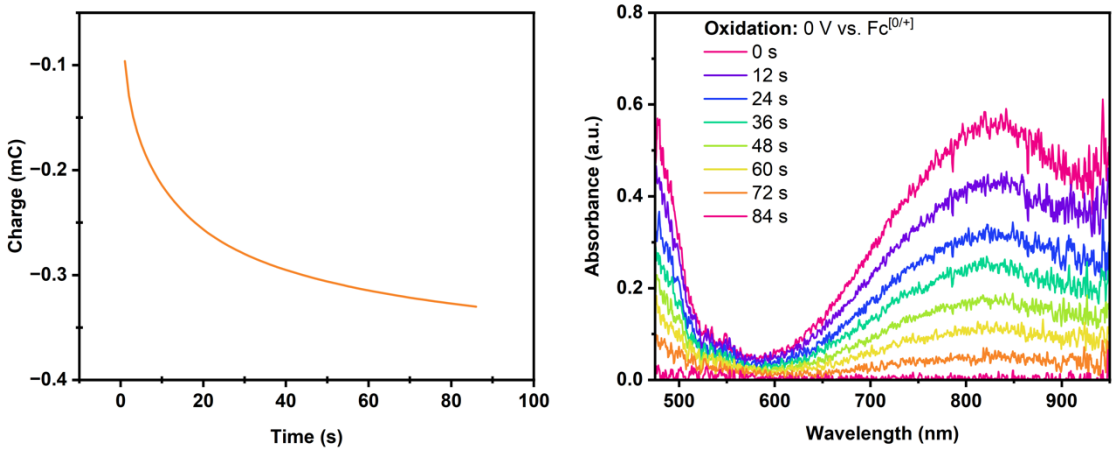

Figure S3. Spectroelectrochemistry data of compound **1** showing (left) the charge passed and (right) the change in spectral absorption profile during subsequent oxidation of this feature, demonstrating its electrochemical reversibility.

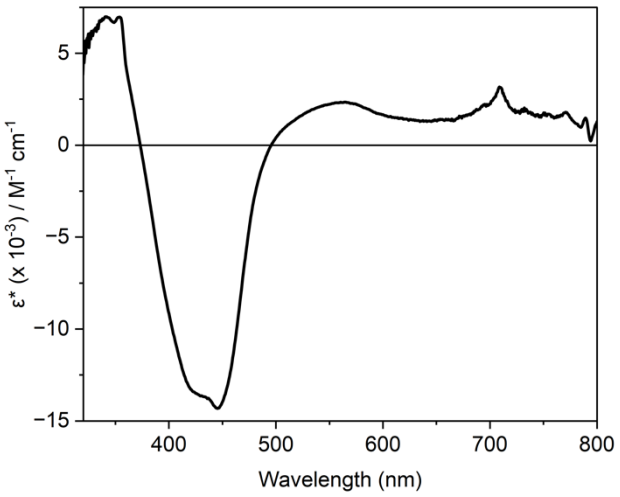

Figure S4. Visible excited state absorption difference spectrum of **2** ($[Ru(phen)_3](PF_6)_2$) monitored at 100 ps (CH_3CN, λ_{ex} = 355 nm, P = 0.2 μJ). The excited state difference spectrum was scaled to an isoabsorbing sample of $[Ru(bpy)_3](PF_6)_2$ ($\varepsilon^*_{GSB,\ 450\ nm} = -1.13 \times 10^4\ M^{-1}\ cm^{-1}$).[1] The feature at 710 nm is a second-order artifact from the 355 nm exciting light source.

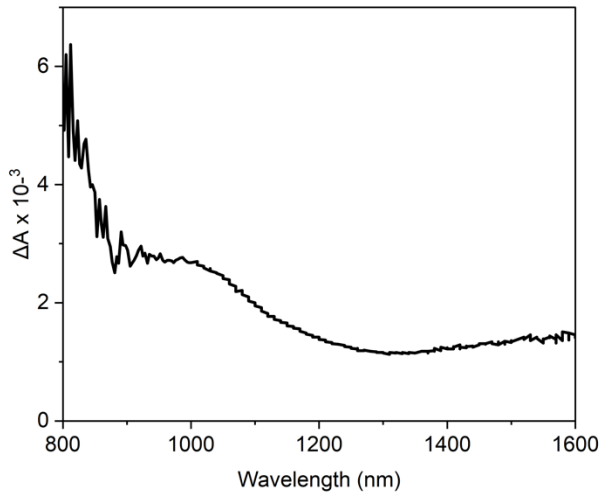

Figure S5. Near-IR excited state absorption difference spectrum of **2** $[Ru(phen)_3](PF_6)_2$ monitored at 100 ps (CH_3CN, λ_{ex} = 355 nm, P = 0.2 μJ).

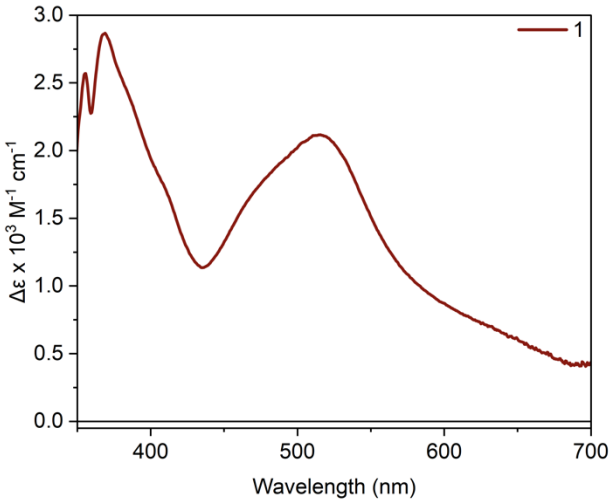

Figure S6. Excited state molar absorptivity of **1** in CH_3CN monitored at 35 ps and referenced to the excited state spectrum of $[Ru(bpy)_3](PF_6)_2$ ($\varepsilon^*_{GSB,\ 448\ nm} = -1.13 \times 10^4\ M^{-1}\ cm^{-1}$).[2]

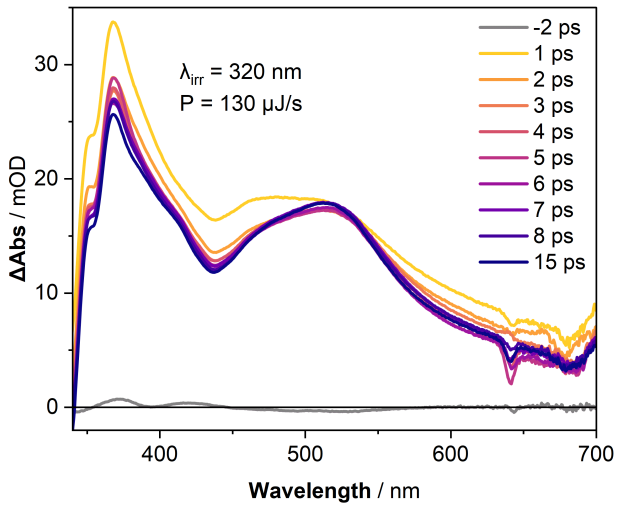

Figure S7. Transient absorption difference spectrum of **1** recorded in CH_3CN following 320 nm excitation. The feature at 640 nm is a second-order artifact from the 320 nm exciting light source.

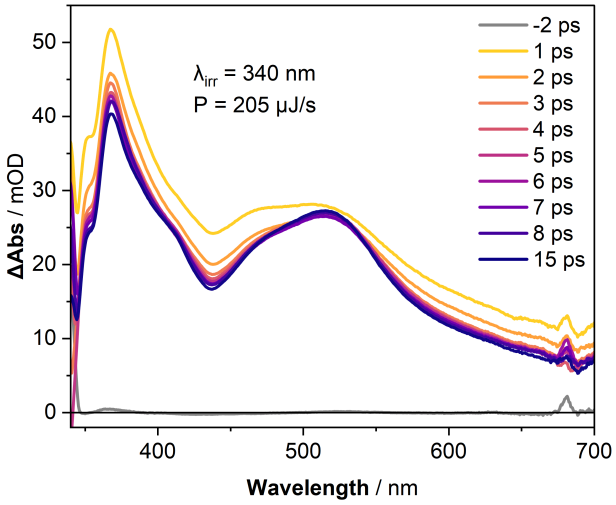

Figure S8. Transient absorption difference spectrum of compound **1** recorded in CH_3CN following 340 nm excitation. The feature at 680 nm is a second-order artifact from the 340 nm exciting light source.

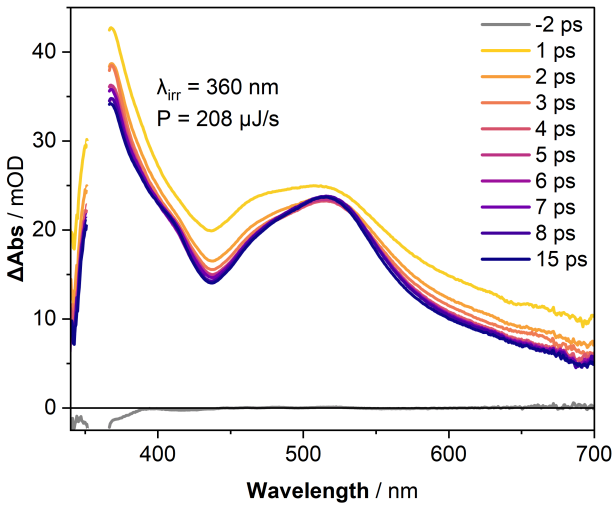

Figure S9. Transient absorption difference spectrum of compound **1** recorded in CH_3CN following 360 nm excitation.

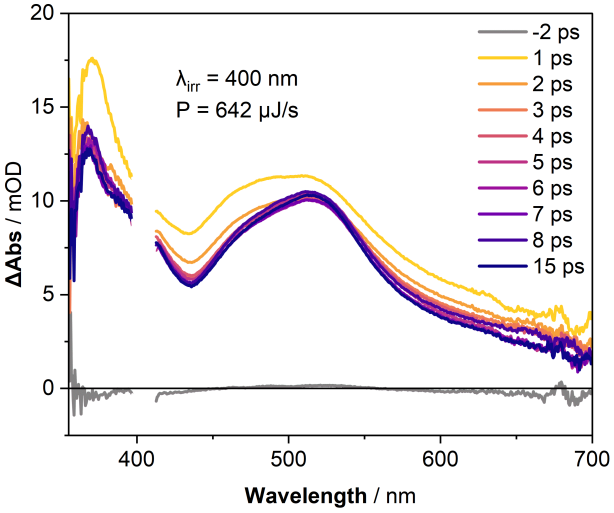

Figure S10. Transient absorption difference spectrum of **1** recorded in CH_3CN following 400 nm excitation.

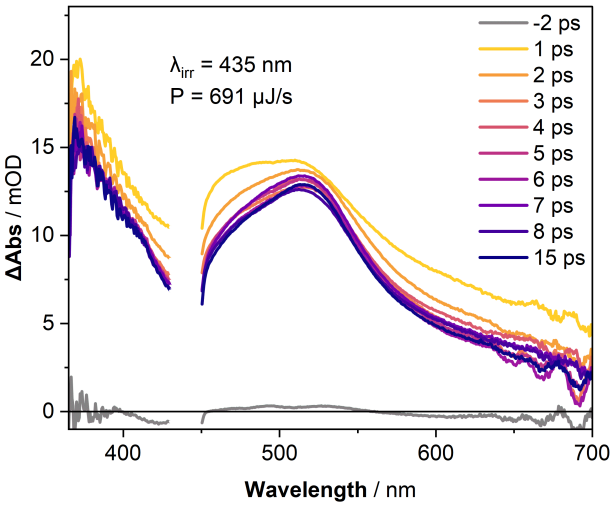

Figure S11. Transient absorption difference spectrum of compound **1** recorded in CH_3CN following 435 nm excitation.

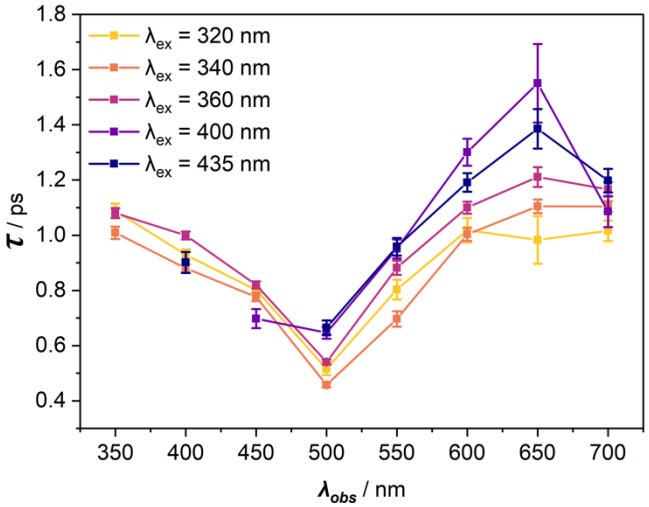

Figure S12. Changes in excited state time constants in **1** measured as a function of excitation wavelength, based on a monoexponential fit. These results match the trends observed by McCusker and coworkers.[2]

Table S1. Vibrational frequencies calculated at B3LYP/def2-SVP level of theory for the quartet ground state. Note that the first six vibrational modes correspond to the first three translational and three rotational degrees of freedom of the molecule and are expected to be close to zero. The structure is confirmed to be a local minimum because all remaining vibrational frequencies are positive

Number	Frequency, cm^{-1}	Intensity, km/mol
1	0	0
2	0	0
3	0	0
4	0	0
5	0	0
6	0	0
7	25,497346	0,16724978
8	25,75534	0,16686269
9	39,9528416	0,14979067
10	40,33414	0,02150099
11	40,4236467	0,02239428
12	42,3552438	0,00011878
13	86,1899495	1,04844619
14	86,2603432	1,05458138
15	92,1774404	0,5018581
16	145,1144191	0,00167972
17	161,6854601	0,58785434
18	162,2214282	0,52487482
19	165,7584631	5,79461726
20	171,6934449	0,01896661
21	171,9824981	0,00335324
22	176,0384981	0,00048679
23	189,7404059	4,18278078
24	190,387474	4,16076996
25	235,823488	2,19671593
26	235,9014848	2,26036744
27	239,7824161	2,00732495
28	273,5414264	0,24154825
29	273,676481	0,23410151
30	283,6054687	0,00016111

31	293,7924668	1,08193492
32	293,88347	1,07390407
33	301,8034368	0,00037014
34	343,9684001	6,59468545
35	354,1734642	30,34731904
36	354,5104005	30,26272634
37	427,4194188	0,08976086
38	427,5324279	0,09353765
39	436,1074628	0,00007927
40	441,4354227	0,00004372
41	447,7314849	17,05428153
42	447,9714872	17,33178012
43	456,4264443	0,02062479
44	464,6694014	9,85177729
45	464,7894548	9,74766776
46	496,8494528	0,08473279
47	496,8794806	0,08612365
48	499,25945	0,03708112
49	523,6104665	3,69018103
50	523,9714402	0,45136598
51	524,0114834	0,46047857
52	532,018444	1,19016976
53	535,0564286	0,26560099
54	535,1404658	0,27375506
55	559,6964617	0,03731299
56	559,7314456	0,0404647
57	562,2284666	0,00001243
58	572,4404501	0,00016655
59	573,6524024	0,11244307
60	573,7164669	0,11413705
61	629,4294757	0,02522866
62	629,4774322	0,02553856
63	634,3424756	0,00024622
64	667,3844163	3,53405205
65	667,449403	3,56840481
66	669,2794631	5,68929774
67	739,4554589	18,90782066
68	739,4664318	8,3510105
69	739,4764777	10,61771089

70	746,5634234	43,07373163
71	748,2044341	47,20297311
72	748,2434777	46,40638881
73	756,529453	50,04197471
74	756,6444835	50,33153779
75	756,9304666	0,37346092
76	796,4064593	4,01713588
77	796,4564232	3,83169597
78	797,2324903	6,3198205
79	821,6314743	0,01535045
80	821,7054991	0,01641394
81	823,4784022	0,00199867
82	879,1864471	46,53514767
83	879,2364253	45,20469837
84	879,5824444	53,75630174
85	888,0424522	0,046278
86	888,1034527	0,05632636
87	888,945408	0,00131016
88	895,6494445	0,00108871
89	897,4224947	39,97128496
90	897,4804607	40,29519246
91	931,1854855	14,01757675
92	931,5434561	3,43752263
93	931,6074573	3,5783223
94	979,4404862	0,02124193
95	979,4854634	0,01437675
96	981,895467	0,02054281
97	982,5654976	5,17554867
98	982,6134743	5,23209208
99	984,8284597	3,80259372
100	1019,414856	0,00020859
101	1019,454826	0,00032428
102	1019,614966	0,00007553
103	1035,554861	0,57639644
104	1035,594399	0,56376582
105	1035,734508	0,5084964
106	1040,024815	0,00008433
107	1040,064023	0,0000633
108	1040,114351	0,00052897

109	1060,274118	1,57077471
110	1063,604103	3,13041868
111	1063,624503	3,15578338
112	1091,514219	5,65739611
113	1091,604268	5,71556431
114	1092,374275	0,02120132
115	1120,394863	0,0150784
116	1120,454624	0,01647317
117	1123,204984	2,37539241
118	1135,674567	47,46382906
119	1135,704139	47,96255035
120	1138,344686	0,00073332
121	1174,62476	23,67619993
122	1174,724415	12,42793687
123	1174,814243	11,74003929
124	1180,114704	2,21238659
125	1180,244184	2,14225054
126	1180,284165	2,54145245
127	1240,234222	7,53211117
128	1240,264146	7,56293545
129	1244,134214	0,00049412
130	1252,244495	0,58454031
131	1252,32426	0,53309833
132	1253,014493	5,99208063
133	1253,054155	5,98771279
134	1253,534639	18,38981586
135	1253,864221	1,31111512
136	1282,754797	0,00416277
137	1282,794835	0,00429213
138	1285,32439	1,74723901
139	1367,194427	28,83900846
140	1367,234361	28,75706387
141	1368,854467	0,03124771
142	1373,904771	0,18529712
143	1374,294683	0,68995242
144	1374,45436	0,59806936
145	1378,714261	3,64552498
146	1378,764542	3,59609484
147	1379,784668	0,00631186

148	1445,074494	35,39545213
149	1446,844491	4,1299262
150	1446,864954	4,06783167
151	1460,404725	84,11345595
152	1460,724277	18,98080661
153	1460,744478	17,55856077
154	1462,534515	13,77861876
155	1462,644888	28,32897745
156	1462,794443	28,29814233
157	1494,014819	17,32408055
158	1494,174578	17,16204644
159	1495,264237	0,19405445
160	1533,684625	18,46931883
161	1534,264968	8,72757359
162	1534,294575	8,76946627
163	1571,534044	126,7550039
164	1571,554747	129,386765
165	1571,564725	9,20835349
166	1627,544212	33,75735123
167	1631,144636	19,54183633
168	1631,184511	19,62436952
169	1633,714863	2,84466076
170	1633,824456	23,60971431
171	1633,86433	25,82103723
172	1644,534895	5,43972329
173	1644,614031	5,77100106
174	1645,114875	33,79759382
175	1675,684938	4,81840577
176	1675,814726	35,58922692
177	1676,014439	30,72452947
178	3212,674213	1,03876294
179	3212,814243	0,88580708
180	3212,834041	1,12264924
181	3213,874608	7,10153544
182	3213,944947	6,79535998
183	3213,994044	5,6296515
184	3214,364464	3,31382524
185	3214,494366	3,48308368
186	3214,534789	3,56239928

187	3223,784668	10,27894621
188	3223,944414	10,53455857
189	3223,994494	8,58071689
190	3227,484175	7,56711855
191	3227,524078	10,21583139
192	3227,724465	3,12752335
193	3227,764996	6,78997192
194	3227,964418	17,61045927
195	3228,224038	6,20395365
196	3237,184607	6,96278835
197	3237,274888	6,42088818
198	3237,394405	6,69503898
199	3237,434306	4,09353688
200	3237,624095	13,00699994
201	3237,85403	5,06419353

Table S2. Calculated transition energies, wavelengths, and oscillator strengths for the quartet electronic states of **1**. Results were obtained using the RASSCF(13,3,3;5,5,7) protocol at the optimized Q_0 geometry, with relative energies referenced to the lowest-lying quartet state.

State	E, eV	E, nm	f	Character
Q_1	2,80	443	7,50E-05	MC
Q_2	2,84	437	7,20E-05	MC
Q_3	2,95	420	2,10E-05	MC
Q_4	3,72	333	1,05E-02	IL+LMCT
Q_5	3,88	319	8,00E-06	MC
Q_6	3,96	313	2,50E-05	MC
Q_7	4,01	309	1,07E-04	MC
Q_8	4,36	284	6,22E-04	MC
Q_9	4,50	276	1,01E-03	LMCT
Q_{10}	4,72	262	1,67E-02	IL
Q_{11}	4,74	261	3,24E-02	IL+LMCT
Q_{12}	4,99	249	1,78E-04	LMCT
Q_{13}	5,00	248	1,22E-03	LMCT

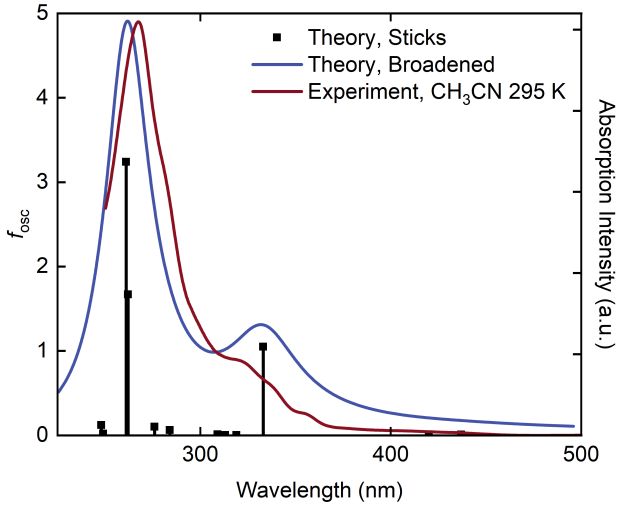

Figure S13. Theoretical absorption spectrum obtained from RASSCF vertical excitations from the ground state quartet, shown with 0.5 eV broadening (blue). The transitions are depicted as sticks with their corresponding oscillator strengths. This is superimposed with the experimental spectrum (red).

Table S3. Calculated transition energies, wavelengths and oscillator strengths and Configuration Interaction (CI) configurations for the doublet electronic states of **1**. Results were obtained using the RASSCF(13,3,3;5,5,7) protocol at the optimized D_1 geometry, with relative energies referenced to the lowest-lying doublet state. The orbital configurations are denoted by their specific spatial orbital occupancies, where 2 indicates a doubly occupied orbital, 0 indicates an unoccupied orbital, u denotes a singly occupied orbital with an up-spin (α) electron, and **d** denotes a singly occupied orbital with a down-spin (β) electron. Only configurations with the highest weights are shown for each state.

State	E, eV	E, nm	f	Main CI coefficients $(\sigma_1)(\sigma_2)(\pi_1)(\pi_2)(\pi_3)$ $(3d_1)(3d_2)(3d_3)(3d_4)(3d_5)$ $(\pi_1^*)(\pi_2^*)(\pi_3^*)(\sigma^*)(4d_1)(4d_2)(4d_3)$	Character
D_2	0,004	-	0	2222220u000000000 2222202u000000000 22222uud000000000	MC
D_3	0,06	19302	0	22222udu000000000 22222uud000000000	MC

				2222220u000000000	
D_4	0,12	10198	0	222222u0000000000 222220u2000000000 22222u02000000000	MC
D_5	0,13	9778	0	22222uud000000000 22222udu000000000 22222u02000000000	MC
D_6	1,02	1213	2,20E-05	22222u20000000000 22222u02000000000 2222202u000000000	MC
D_7	1,04	1197	2,80E-05	2222202u000000000 2222220u000000000 22222u02000000000	MC
D_8	1,14	1088	7,00E-06	222220u2000000000 222222u0000000000 2222u2u000d000000	MC
D_9	2,14	579	2,70E-05	22222ud00u0000000 22222u0du00000000 222220udu00000000	MC
D_{10}	2,40	517	1,50E-05	22222uu00d0000000 222220uud00000000 222220200u0000000	MC
D_{11}	2,43	511	5,40E-05	222220uu0d0000000 22222u0u0d0000000 222220ud0u0000000	MC
D_{12}	2,50	495	2,00E-06	22222u0ud00000000 222220uud00000000 222220200u0000000	MC
D_{13}	2,53	490	1,00E-05	222220200u0000000 22222u0ud00000000	MC

				222220udu00000000	
D_{14}	2,56	485	1,40E-05	222220ud0u0000000 22222020u00000000 22222uu0d00000000	MC
D_{15}	2,60	477	2,00E-05	22222u0du00000000 22222002u00000000 22222200u00000000	MC
D_{16}	2,81	441	1,10E-05	22222u0du00000000 22222ud00u0000000 222220200u0000000	MC
D_{17}	2,83	438	2,40E-05	22222002u00000000 22222u0d0u0000000 22222ud0u00000000	MC
D_{18}	3,26	380	1,10E-05	22222u0u0d0000000 222220uu0d0000000 22222002u00000000	MC
D_{19}	3,29	377	0	u2222duu00000000d u2222udu00000000d u2222uud00000000d	MLCT
D_{20}	3,33	373	9,00E-06	22222u0ud00000000 22222uu00d0000000 222220uud00000000	MC
D_{21}	3,36	369	1,21E-04	222u2duu000d00000 222u2udu000d00000 222u2uud000d00000 222220uu0d0000000	IL+MC
D_{22}	3,37	368	8,00E-06	22222uu0d00000000 222220uud00000000 222220uu0d0000000	MC+IL
D_{23}	4,09	303	1,10E-05	222220020u0000000	MC

				22222u0d0u0000000 22222ud00u0000000	
D_{24}	4,14	299	9,00E-06	222220udu00000000 22222200u00000000 22222020u00000000	MC
D_{25}	4,18	297	2,30E-05	22222020u00000000 22222u0du00000000 222220udu00000000	MC
D_{26}	4,38	283	1,03E-04	22222ud0u00000000 22222u0d0u0000000 222220ud0u0000000	MC
D_{27}	4,88	254	2,00E-06	222220u0du0000000 22222u00ud0000000 222220u0ud0000000	MC
D_{28}	4,93	252	4,00E-06	222220u0du0000000 22222u00du0000000 22222u00ud0000000	MC
D_{29}	4,93	251	2,00E-06	2222200udu0000000 2222200uud0000000 222220u0020000000	MC
D_{30}	5,07	244	1,00E-05	222220u0020000000 22222u00020000000 2222200uud0000000	MC

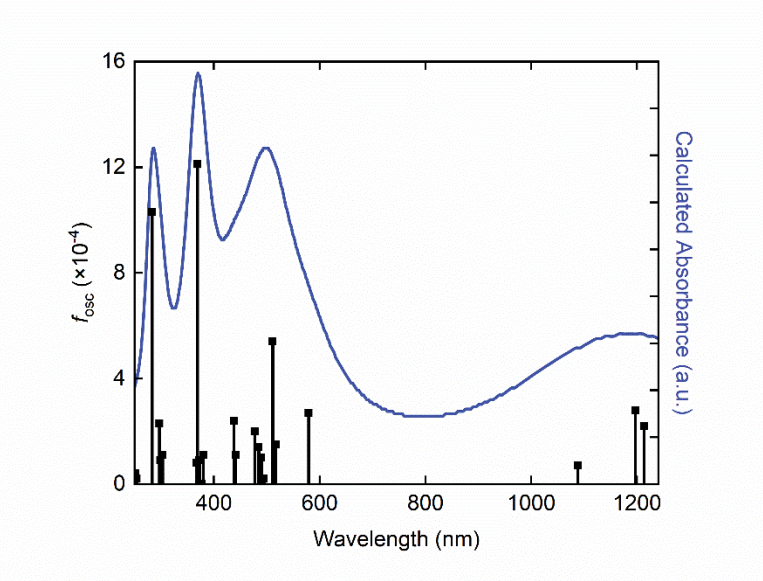

Figure S14. Theoretical absorption spectrum obtained from RASSCF vertical excitations from the doublet minima, shown with 0.5 eV broadening. The transitions are depicted as sticks with their corresponding oscillator strengths.

Table S4. Multi-state CASPT2 (MS-CASPT2) relative energies for the quartet and doublet electronic states of **1**. Calculations utilized an IPEA shift of 0.25 a.u. and an imaginary shift of 0.4 a.u. to ensure convergence and minimize intruder state effects. A CASSCF(3,5) wavefunction was employed, with state-averaging performed over five quartet states and four doublet states. All calculations were conducted at the optimized D_1 geometry, with relative energies referenced to the doublet minima.

State	E, eV
Q_0	-1,97
D_1	0,00
D_2	0,03
D_3	0,09
D_4	0,13
D_5	0,14
Q_2	0,27
Q_3	0,34
Q_4	0,38

2. Synthesis and Characterization Data

Synthesis of chromium(III) *tris*(1,10-phenanthroline) *tris*(tetrafluoroborate) (1)

The complex was prepared in a nitrogen-filled glovebox. In a 20 mL scintillation vial, a blue solution of $[Cr(CH_3CN)_4](BF_4)_2$ (100.0 mg, 0.256 mmol, 1 equiv) in 2 mL CH_3CN was prepared. The 1,10-phenanthroline ligand (143.3 mg, 0.795 mmol, 3.1 equiv) was dissolved in 4 mL of 1:1 CH_3CN:DCM in a second 20 mL scintillation vial, then added to the metal solution, generating a dark brown or green mixture that was stirred for 1 hour. Solid $AgBF_4$ was dissolved in minimal CH_3CN and added to the mixture, generating a yellow-orange solution that was stirred in the glovebox in the dark for 12 hours. The precipitated Ag^0 solid waste was discarded after filtration through a PTFE syringe filter (0.25 µm), leaving a yellow solution. Initial purification was achieved by precipitation in 10 mL Et_2O, followed by filtration through a fine frit and washing twice with 2 mL Et_2O. Single crystals were obtained via Et_2O/CH_3CN vapor diffusion at room temperature, yielding 128.5 mg of yellow, needlelike crystals (59% yield).

HRMS (ESI): m/z $[M - 3\ BF_4]^{3+}$, calcd for $[CrC_{36}H_{24}N_6]^{3+}$: 197.3817; found: 197.3823 (Δ = 3.0 ppm). Elemental analysis (%): Calculated for $CrC_{36}H_{24}N_6B_3F_{12}\cdot 0.5\ CH_2Cl_2$: C, 48.96; H, 2.81; N, 9.38. Found: C, 48.89; H, 3.05; N, 9.40.

Synthesis of ruthenium(II) *tris*(1,10-phenanthroline)$_3$ *bis*(hexafluorophosphate) (2)

To a 100 mL round-bottom flask were added 131 mg of $RuCl_3\cdot 3H_2O$ (1 eq.), 275 mg (3 eq.) of 1,10-phenanthroline, 20 mL of ethylene glycol, and a magnetic stir bar. The resultant black mixture was refluxed under a nitrogen atmosphere for 3 h. The solution changed color from black to bright orange/red over the course of the reaction. The reaction solution was cooled to room temperature and added to a saturated, 150 mL solution of NH_4PF_6 (aq.), forming a bright orange precipitate. The precipitate was collected by vacuum filtration and washed with 50 mL of ice-cold ethanol. The product was dried in a vacuum oven at 40 °C overnight, resulting in a light-orange powder (415 mg, 89% yield).

^{1}H NMR (400 MHz, CD_3CN) δ 8.62 (d, J = 8.1 Hz, 6H), 8.27 (s, 6H), 8.03 (d, J = 5.3 Hz, 6H), 7.65 (dd, J = 8.4, 5.3, 6H).

3. UV-Visible Spectroscopy

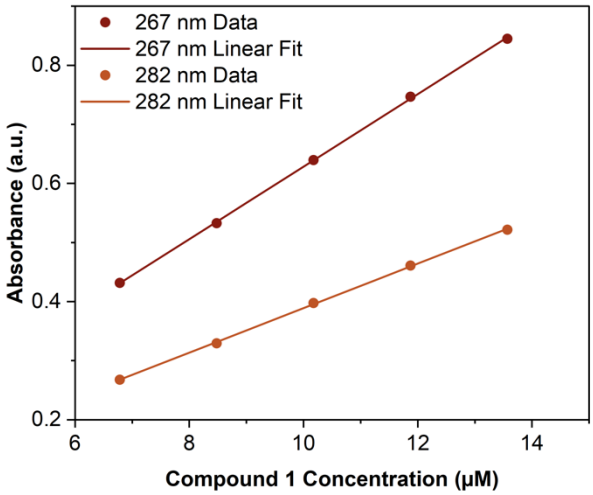

Figure S15. Molar extinction plots for compound **1** at 267 and 282 nm. Absorbance values were obtained at five concentrations (6.78 – 13.57 μM) in CH_3CN solvent. Linear fits yield molar absorption coefficients of 6.13×10^4 M^{-1} cm^{-1} (267 nm) and 3.77×10^4 M^{-1} cm^{-1} (282 nm), with $R^2 > 0.9995$ in both cases.

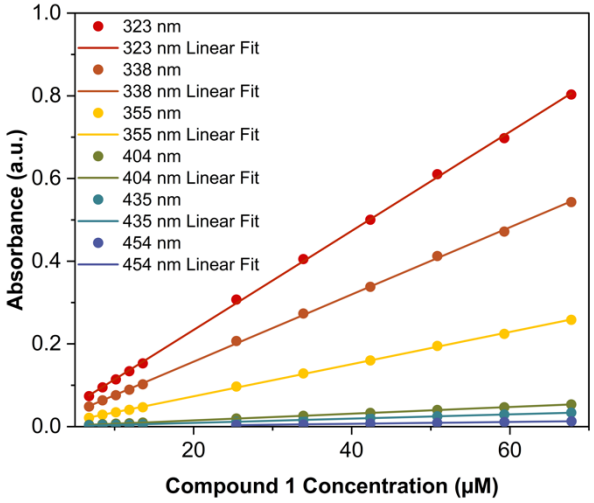

Figure S16. Molar extinction plots for compound **1** from 323 to 454 nm. Absorbance values for 323 nm to 435 nm were obtained at eleven concentrations (6.78 – 67.8 μM) in CH_3CN solvent. Linear fits yield molar absorption values of 1.20×10^4 M^{-1} cm^{-1} (323 nm), 8.12×10^3 M^{-1} cm^{-1} (338 nm), 3.89×10^3 M^{-1} cm^{-1} (355 nm), 809 M^{-1} cm^{-1} (404 nm), 513 M^{-1} cm^{-1} and (435 nm) with $R^2 > 0.9995$ in all cases. Data for 219 M^{-1} cm^{-1} (454 nm) was obtained at six concentrations (25.4 – 67.8 μM) in CH_3CN solvent with $R^2 > 0.9994$.

4. Infrared Spectroscopy

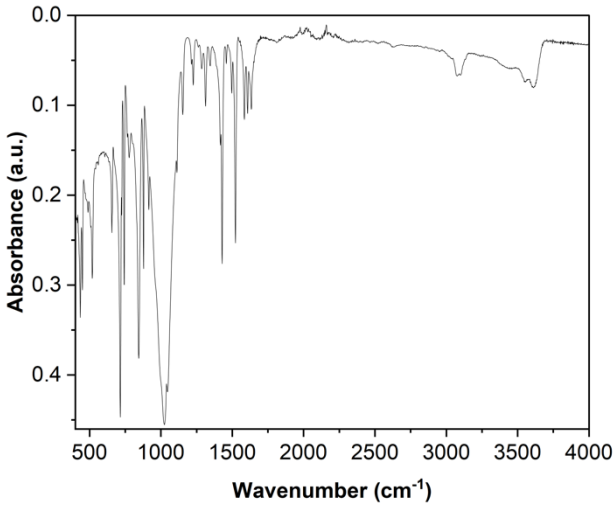

Figure S17. Full (400 to 4000 cm^{-1}) solid-state ATR-IR spectrum of **1**.

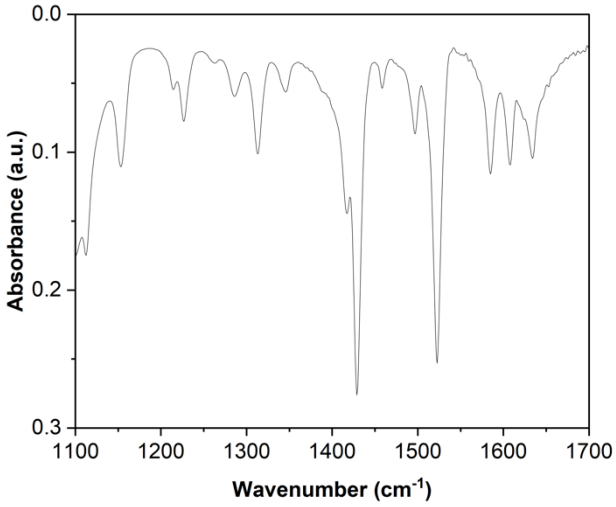

Figure S18. Partial (1100 to 1700 cm^{-1}) solid-state ATR-IR spectrum of **1**.

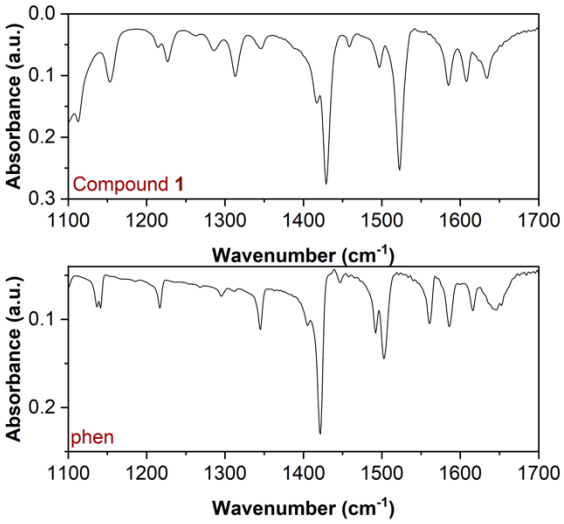

Figure S19. Comparison of ligand breathing modes between **1** (top) and the 1,10-phenanthroline ligand (bottom), recorded using solid-state ATR-IR.

5. Electrochemistry Measurements

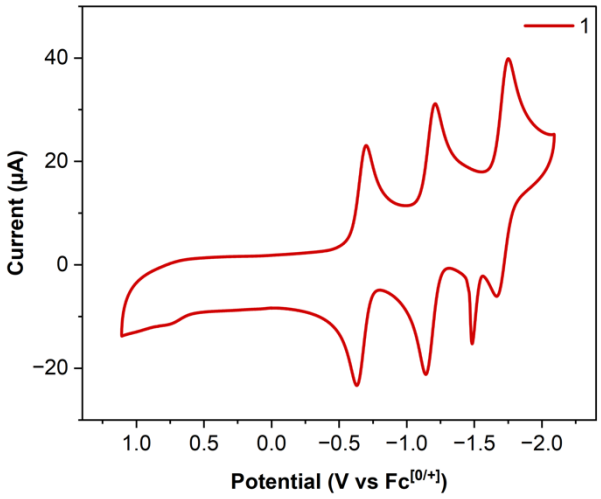

Figure S20. Cyclic voltammetry data for **1** (0.1 mM) recorded in CH_3CN with 0.25 M [^{n}Bu$_4$][PF_6] supporting electrolyte at 100 mV/s scan rate. The sharp feature at -1.5 V vs $Fc^{[0/+]}$ in the anodic scan reflects electrode surface deposition, which disappears at higher scan rates.

Table S6. Electrochemical reduction potentials of **1**. Potentials measured at the half-wave potential ($E_{1/2}$) and reported versus $Fc^{[0/+]}$. Measurements recorded with 0.1 mM sample in 0.25 M [^{n}Bu$_4$][PF_6] supporting electrolyte using CH_3CN solvent. Measurements made at 100 mV/s scan rate. Reductions correspond to the following formal transitions: $[CrL_3]^{3+}/[CrL_2(L^{\bullet-})]^{2+}$, $[CrL_2(L^{\bullet-})]^{2+}/[CrL(L^{\bullet-})_2]^{1+}$, etc.

Species	*E*(3+/2+)	*E*(2+/1+)	*E*(1+/0)	*E*(0/1−)
1	−0.67	−1.18	−1.71	–

6. Transient Absorption Spectroscopy

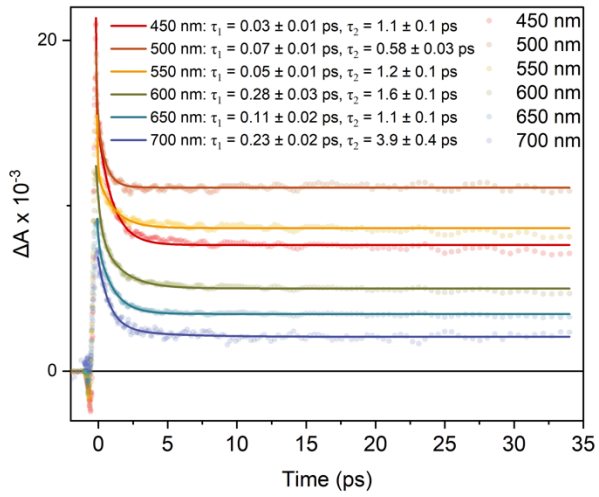

Figure S21. Kinetic traces of the transient absorption spectrum of **1** measured in CH_3CN at RT.

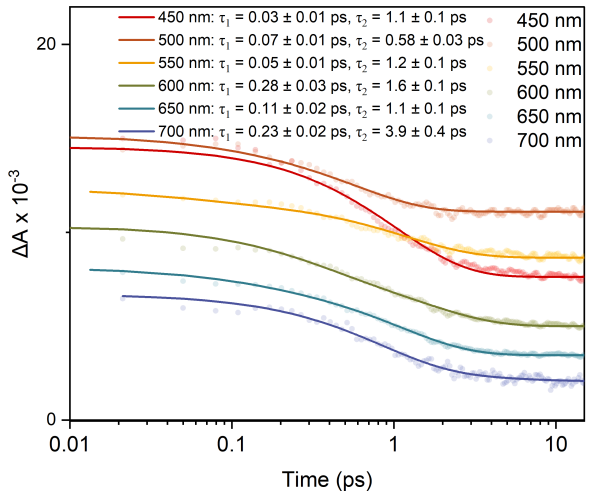

Figure S22. Kinetic traces of the transient absorption spectrum of **1** measured in CH_3CN at RT. The logarithmic time axis shows the excited-state evolution up to 15 ps.

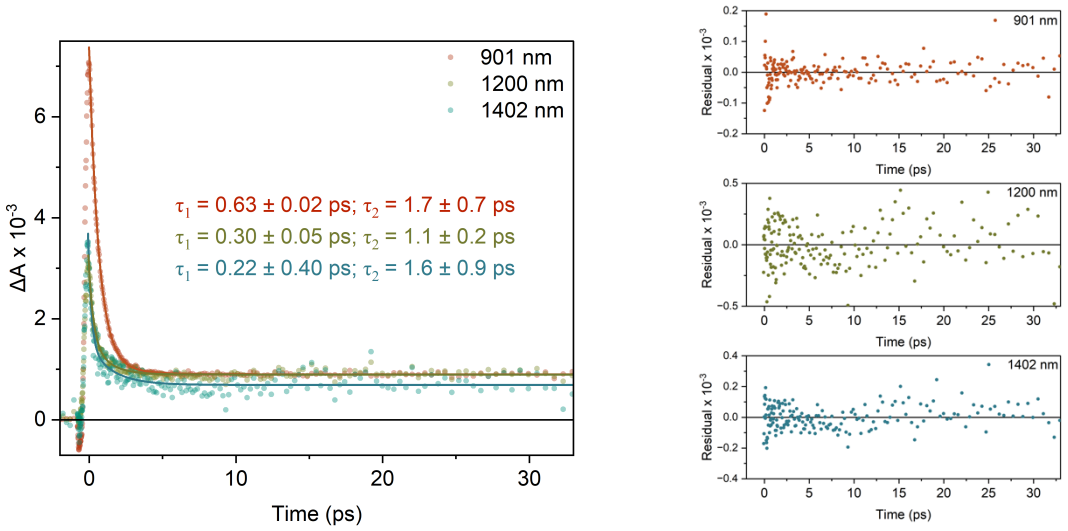

Figure S23. Kinetic traces and residuals of the transient absorption kinetics of **1** measured in CH_3CN at RT.

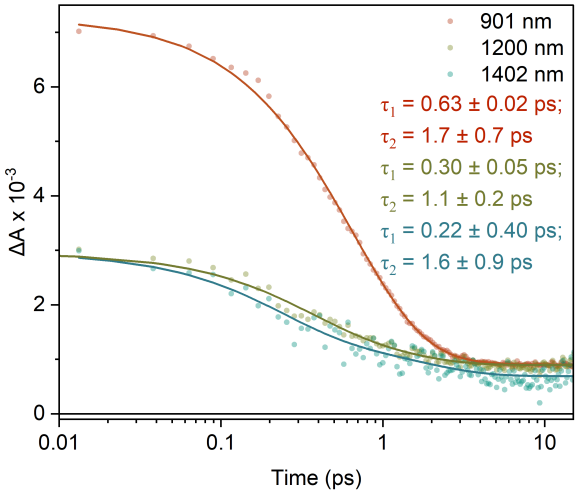

Figure S24. Kinetic traces and residuals of the transient absorption kinetics of **1** measured in CH_3CN at RT. The logarithmic time axis shows the excited state evolution up to 15 ps.

7. Time-Resolved PL Emission

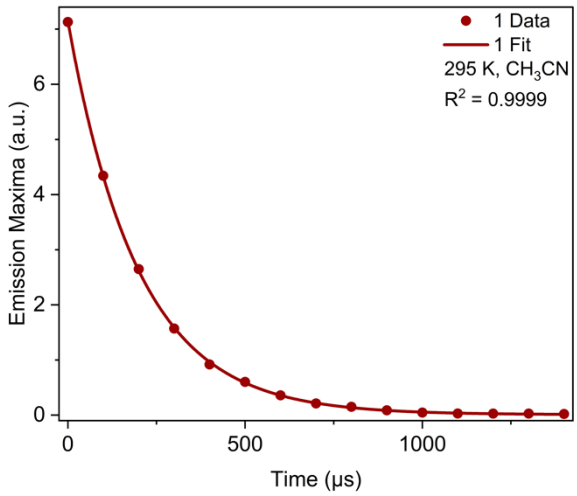

Figure S25. Nanosecond emission measurements of **1**, recorded from the ^{2}E PL emission feature (Abs = 0.496 a.u. at 355 nm, 295 K, CH_3CN).

8. Optimized Structures

Optimized Quartet Minima (Q_0) of compound 1, Å

Cr	0.002311	-0.008669	0.005767
N	0.187471	1.749734	1.077650
C	1.137868	2.576721	0.548073
C	1.434246	3.848184	1.097229
C	0.689430	4.248359	2.235045
C	-0.276648	3.400049	2.755686
C	-0.502299	2.152460	2.148303
C	2.457716	4.650156	0.483126
H	0.879004	5.218436	2.693214
H	-0.862514	3.684278	3.627020
H	-1.253654	1.470915	2.540181
N	1.421877	-1.030531	1.107019
N	-1.604623	-0.699688	1.107406
N	1.507608	0.882705	-1.096960
N	-1.531375	0.830329	-1.099843
N	0.031979	-1.775034	-1.069285
C	1.848066	2.110641	-0.603791
C	1.665315	-2.276781	0.602137
C	2.111592	-0.613821	2.172508
C	-2.799705	-0.284456	0.591137
C	-1.599908	-1.479015	2.192258
C	2.156952	0.406587	-2.162858
C	-2.760287	0.538493	-0.579031
C	-1.452033	1.602046	-2.187431
C	0.916542	-2.677678	-0.549852
C	-0.692145	-2.114940	-2.139154
C	2.857021	2.914314	-1.188777
C	2.613637	-3.159554	1.174020
C	3.077103	-1.420916	2.799204
H	1.895845	0.385213	2.544067
C	-4.043840	-0.634954	1.169885
C	-2.787785	-1.879518	2.828736
H	-0.631186	-1.794552	2.572735
C	3.177179	1.132839	-2.801735
H	1.861953	-0.574708	-2.527177
C	-3.964629	1.012572	-1.154056
C	-2.595461	2.119039	-2.821109
H	-0.458117	1.817040	-2.572915
C	1.111433	-3.963661	-1.110397
C	-0.568147	-3.372184	-2.755722
H	-1.388081	-1.373356	-2.524166
C	3.527288	2.385857	-2.320528
C	3.142410	4.200934	-0.613505
C	3.328574	-2.692716	2.305566

C	2.797743	-4.459043	0.586404
H	3.613730	-1.037990	3.664468
C	-4.008984	-1.458239	2.323290
C	-5.254189	-0.144567	0.567964
H	-2.733768	-2.513645	3.710907
H	3.677485	0.703799	-3.667152
C	-3.851026	1.825580	-2.309629
C	-5.216133	0.648366	-0.546862
H	-2.481046	2.741462	-3.705881
C	0.332189	-4.296535	-2.246772
C	2.074216	-4.846251	-0.508971
H	-1.178714	-3.603191	-3.625819
H	4.312480	2.965406	-2.804792
H	4.071147	-3.333613	2.779585
H	-4.939678	-1.755822	2.805095
H	-4.748634	2.215017	-2.788753
H	0.444019	-5.274543	-2.713575
H	2.681711	5.626828	0.908685
H	3.916951	4.816151	-1.068134
H	2.220562	-5.833692	-0.943261
H	3.526278	-5.134837	1.030957
H	-6.139349	1.015096	-0.992166
H	-6.208099	-0.415612	1.017025

Optimized Doublet Minima (D_1) of compound 1, Å

Cr	0.003890	-0.007141	0.003400
N	0.228565	1.795933	1.073930
C	1.169805	2.618487	0.544565
C	1.464411	3.864630	1.076747
C	0.728879	4.274398	2.206981
C	-0.225561	3.448777	2.727376
C	-0.444052	2.210653	2.124107
C	2.485376	4.672582	0.472083
H	0.923046	5.234088	2.650829
H	-0.806466	3.729484	3.584384
H	-1.188508	1.548195	2.520881
N	1.448304	-1.082273	1.108321
N	-1.664016	-0.690698	1.108971
N	1.537322	0.938912	-1.105465
N	-1.592960	0.824882	-1.101964
N	0.066970	-1.820813	-1.070118
C	1.877177	2.155720	-0.609768
C	1.688810	-2.319357	0.604192
C	2.137359	-0.690397	2.156102
C	-2.850622	-0.282636	0.592199
C	-1.678737	-1.461967	2.172658
C	2.190162	0.487221	-2.152262
C	-2.812107	0.537273	-0.579746
C	-1.535447	1.591114	-2.168046
C	0.942552	-2.718151	-0.549467
C	-0.641837	-2.175581	-2.118346
C	2.865194	2.948896	-1.173243
C	2.612840	-3.191455	1.159478
C	3.092442	-1.491431	2.782025
H	1.937409	0.293937	2.532735
C	-4.072643	-0.625372	1.150650
C	-2.855315	-1.866564	2.803131
H	-0.729921	-1.780133	2.559170
C	3.203695	1.206274	-2.785967
H	1.911561	-0.480340	-2.522392
C	-3.996296	0.998755	-1.134267
C	-2.668539	2.109174	-2.794799
H	-0.561466	1.812372	-2.559304
C	1.135320	-3.980752	-1.089350
C	-0.524924	-3.424082	-2.728645
H	-1.333685	-1.454352	-2.507796
C	3.539398	2.436796	-2.300156
C	3.158250	4.232813	-0.601933
C	3.328752	-2.741299	2.287135
C	2.801549	-4.491048	0.579741

H	3.621204	-1.114748	3.635984
C	-4.051023	-1.446870	2.295758
C	-5.286588	-0.141844	0.556088
H	-2.801464	-2.495703	3.670326
H	3.698350	0.783581	-3.638836
C	-3.897907	1.811890	-2.281233
C	-5.249899	0.638360	-0.534622
H	-2.556122	2.727595	-3.664079
C	0.364141	-4.325092	-2.217731
C	2.091857	-4.870123	-0.493744
H	-1.130775	-3.653676	-3.583597
H	4.313935	3.017147	-2.768088
H	4.056575	-3.383900	2.748668
H	-4.975286	-1.738922	2.760667
H	-4.790517	2.193503	-2.743104
H	0.479731	-5.294706	-2.667389
H	2.701435	5.634320	0.898345
H	3.925050	4.834683	-1.052593
H	2.229513	-5.843511	-0.926049
H	3.520033	-5.154244	1.023897
H	-6.157290	1.003384	-0.978158
H	-6.224017	-0.415348	1.003024

References

1. P. Müller and K. Brettel, "$[Ru(bpy)_3]^{2+}$ as a reference in transient absorption spectroscopy: differential absorption coefficients for formation of the long-lived ^{3}MLCT excited state."*Photochem Photobiol Sci*, 2012, **11**, 632–636.
2. E. A. Juban, *The Ultrafast Dynamics of Chromium (III) Coordination Complexes*, University of California, Berkeley, 2006.